

A Complete *E*-Plane Analysis of Waveguide Junctions Using the Finite Element Method

VASSILIOS N. KANELLOPOULOS AND J. P. WEBB, MEMBER, IEEE

Abstract—A complete finite element analysis of inhomogeneous *E*-plane waveguide junctions is presented. It is shown that at least two field components are needed for the analysis. This method solves for the three components of the magnetic field in two dimensions, and calculates the scattering parameters of the junction. Precalculated matrices are used for fast matrix assembly. Results for a metallic post agree very well with earlier published values. A dielectric post was also analyzed.

I. INTRODUCTION

OF THE NUMERICAL methods available for determining the scattering parameters of a waveguide junction, certain computer techniques have the advantage that they can handle arbitrarily shaped regions. However the general waveguide junction is three-dimensional and its analysis with these techniques requires a considerable effort in order to define the geometry of the problem in three dimensions, as well as a great deal of computer memory and time. It is worthwhile, therefore, to consider some useful subclasses of problems which are essentially two-dimensional. In these problems, the variation of the field is known in one coordinate direction and the analysis can be done in two dimensions. For the case of rectangular waveguide junctions, there are two major categories of problems that can be analyzed in two dimensions [1]:

- i) analysis in the *H* plane [2]–[8] (*H*-plane junctions),
- ii) analysis in the *E* plane (*E*-plane junctions).

Interest in *E*-plane junctions was first shown by Lewin in the late 1940's [9]. More recent papers on *E*-plane junctions include [10] and [12]–[14]. Examples of *E*-plane junctions are *E*-plane bends; T junctions; capacitive posts and irises [1]; tapers and transitions from one width to another [9]; phase shifters; filters [15], [16]; and power dividers [17]. Lately, there has been interest in the applications of the nonradiative dielectric (NRD) waveguide T junction in microwave and millimeter-wave integrated circuits [18]. The analysis of this is closely related to that of an *E*-plane rectangular waveguide junction.

In homogeneous *E*-plane problems, there is no *x* component of electric field, and a scalar formulation in terms of H_x is possible, very similar to the E_y formulation for

Manuscript received April 2, 1988; revised October 26, 1989. This work was supported by the Natural Sciences and Engineering Research Council of Canada and the Centre de Recherche Informatique de Montréal.

The authors are with the Computational Analysis and Design Laboratory, Department of Electrical Engineering, McGill University, 3480 University Street, Montréal, H3A 2A7, Canada.

IEEE Log Number 8933245.

H-plane problems. This has prompted some authors [6], [10] to claim that *E*-plane junctions can in general be treated in much the same way as *H*-plane junctions. However in *E*-plane problems involving dielectric obstacles, E_x is not zero, despite the fact that this component is not present in the incident TE_{10} wave. This fact was pointed out by Schwinger and Saxon [5] and is shown mathematically in the following section. A consequence, also demonstrated in the next section, is that the analysis of a general, inhomogeneous *E*-plane junction involves at least two, coupled variables. Koshiba *et al.* [10] managed to analyze *E*-plane junctions as scalar problems, but their method works only in two special cases: a) an inhomogeneous junction of parallel-plate waveguides where the excitation is a TEM mode, and b) a homogeneous *E*-plane junction of rectangular waveguides. Their method cannot correctly analyze the inhomogeneous *E*-plane junction.

In this paper, we present a new method which is not restricted in this way. The method can analyze arbitrarily shaped, inhomogeneous *E*-plane junctions. It was successfully tested with various simple problems where analytical solutions were available. It was also used to find the scattering coefficients of more complicated problems. Here, we present results of the analysis of *E*-plane metallic and dielectric posts in rectangular waveguides. Our results agree very well with those published for a metallic post in [1]. However, no comparison was possible for the case of the dielectric post, since no results have been published previously for this case.

II. MATHEMATICAL FORMULATION FOR *E*-PLANE JUNCTIONS

The analysis of *E*-plane junctions takes place in the plane of the electric field of the dominant mode of the waveguides. The junction is translationally symmetric along the *x* coordinate direction. It is assumed that only the dominant mode TE_{10} can propagate in each waveguide, and is incident upon the junction.

It is known that in the junction (Fig. 1) higher modes are excited so that the field satisfies the boundary conditions on the conductors and dielectric interfaces. The ports (Fig. 1) are defined as reference planes far away from the junction, where it is assumed that all the higher modes have been strongly attenuated and only the dominant mode is present. This attenuation is due to the fact that the

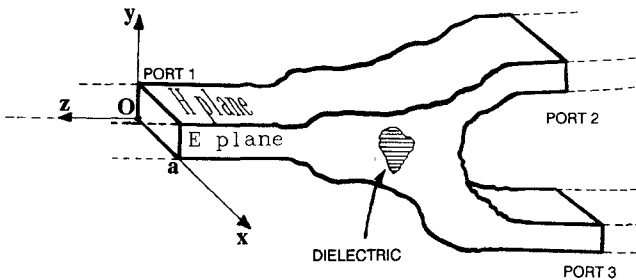


Fig. 1. A three-port inhomogeneous *E*-plane junction of rectangular waveguides.

rectangular waveguides connected to the junction can support only the dominant mode. Because of the existing translational symmetry of the junction, the variation of the electromagnetic field in the *x* direction is the same as that of the dominant mode (which is known). Thus, only the TE_{1n} ($n = 0, 1, 2, \dots$) and TM_{1m} ($m = 1, 2, \dots$) modes can be excited. The analysis, therefore, can be carried out in two dimensions *y* and *z*, and the magnetic field can be expressed as

$$\begin{aligned} H_x(x, y, z) &= H_x(y, z) \sin\left(\frac{\pi}{a}x\right) \\ H_y(x, y, z) &= H_y(y, z) \cos\left(\frac{\pi}{a}x\right) \\ H_z(x, y, z) &= H_z(y, z) \cos\left(\frac{\pi}{a}x\right) \end{aligned} \quad (1)$$

where *a* is the broad dimension of the waveguides.

A. Homogeneous *E*-Plane Junction: The Scalar Problem

In this case only one dielectric material is present in the junction; i.e., ϵ_r is constant everywhere in the junction and no dielectric interfaces are present. Then, the problem can be solved with just one component (H_x). This is shown below.

The vector Helmholtz equation for the magnetic field can be rewritten as

$$\nabla_t^2 \mathbf{H}_t + k_t^2 \mathbf{H}_t = 0 \quad (2a)$$

$$\nabla_t^2 H_x + k_t^2 H_x = 0 \quad (2b)$$

where the subscript *t* denotes the component in the *y*-*z* plane and k_t is given by the expression

$$k_t^2 = \epsilon_r k_0^2 - \left(\frac{\pi}{a}\right)^2 \quad (2c)$$

with ϵ_r being the relative permittivity of the medium and k_0 the normalized frequency, ω/c , where ω is the angular frequency and c the velocity of light in vacuum.

The scalar equation (2b) gives a unique solution for H_x alone, when the following boundary conditions are applied:

$$H_x = H_0 \quad \text{or} \quad \frac{\partial H_x}{\partial n} = 0. \quad (2d)$$

An expression similar to (2b) holds for the *x* component of

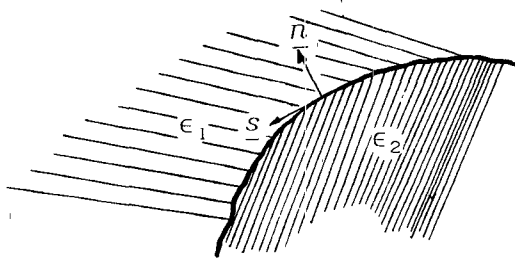


Fig. 2. A dielectric interface.

the electric field:

$$\nabla_t^2 E_x + k_t^2 E_x = 0 \quad (3)$$

where again a unique solution is provided for E_x with

$$E_x = E_0 \quad \text{or} \quad \frac{\partial E_x}{\partial n} = 0 \quad \text{on the boundaries.}$$

However, for the *E*-plane junction, we know that $E_0 = 0$ at the ports. Thus, $E_x = 0$ everywhere in the junction.

It can be shown that the *y*-*z* (denoted as *t*) magnetic field component is given by

$$\mathbf{H}_t = \frac{1}{k_t^2} \left(\frac{\pi}{a} \nabla_t H_x + j\omega \epsilon_r \epsilon_0 \nabla_t E_x \times \mathbf{a}_x \right) \quad (4)$$

where \mathbf{a}_x is the unit vector in the *x* direction. Since $E_x = 0$, equation (4) reduces to

$$\mathbf{H}_t = \frac{1}{k_t^2} \left(\frac{\pi}{a} \nabla_t H_x \right). \quad (5)$$

Thus, once H_x has been computed, the rest of the magnetic field can be found from it.

B. Inhomogeneous *E*-Plane Junction: The Vector Problem

In this case, more than one region of constant permittivity ϵ_r is present in the junction and dielectric interfaces exist over the *E* plane. (A continuously varying ϵ_r could be modeled as a piecewise-constant permittivity.) It will be shown that, in general, the dielectric interfaces excite the E_x component of the electric field, which is coupled to the H_x component of the magnetic field. Thus, the analysis in this case cannot be done in just one variable (H_x).

At the dielectric interface shown in Fig. 2, let \mathbf{n} and \mathbf{s} be unit normal and tangential vectors respectively. If we assume that E_x is zero everywhere in the junction, as we did for the homogeneous case, then the *y*-*z* component of the magnetic field is given by (5). Since the tangential component of the transverse magnetic field is continuous across dielectric interfaces, the right-hand side of the following equation should be continuous too:

$$\mathbf{H}_t \cdot \mathbf{s} = \frac{1}{k_t^2} \left(\frac{\pi}{a} \nabla_t H_x \cdot \mathbf{s} \right). \quad (6)$$

The term in the brackets is indeed continuous. However the parameter k_t is not because it depends on the permittivity (see (2c)). Therefore, (5) is not valid and the assumption that E_x is zero is wrong. Thus, we come to the conclusion that at dielectric interfaces the component E_x of the electric field is excited in order for the interface conditions to be satisfied.

Further, not only are H_x and E_x both nonzero, but they are coupled together. This can be shown from the continuity condition of the magnetic field across the interfaces:

$$\mathbf{H}_t \cdot \mathbf{n}|_{\epsilon_1} = \mathbf{H}_t \cdot \mathbf{n}|_{\epsilon_2}. \quad (7)$$

After some algebra, this gives

$$\frac{1}{k_{t_1}^2} \frac{\partial H_x}{\partial n} \Bigg|_{\epsilon_1} - \frac{1}{k_{t_2}^2} \frac{\partial H_x}{\partial n} \Bigg|_{\epsilon_2} = j\omega\epsilon_0 \frac{a}{\pi} \frac{\partial E_x}{\partial s} \left(\frac{\epsilon_{r_2}}{k_{t_2}^2} - \frac{\epsilon_{r_1}}{k_{t_1}^2} \right). \quad (8)$$

From the above equation we can see that the behavior of H_x across an interface depends on the change of E_x along that interface.

Note that (2b) is still correct in each uniform region, and the boundary conditions (2d) still hold. However,

$$\frac{\partial H_x}{\partial n}$$

is no longer continuous (from (8)), so (2b) and (2d) are not sufficient to determine H_x .

Although two variables, H_x and E_x , are sufficient, the new method uses the three components of the magnetic field as the unknowns. The three-component approach has been shown to be very successful in the analysis of waveguide modes [20].

III. FINITE ELEMENT ANALYSIS AND THE COMPUTER PROGRAM

For linear, nonmagnetic, isotropic, lossless materials and for time-harmonic fields the suggested functional is [21]

$$F(\mathbf{H}) = \int_V \left\{ (\nabla \times \mathbf{H}^*) \frac{1}{\epsilon_r} (\nabla \times \mathbf{H}) - k_0^2 \mathbf{H}^* \cdot \mathbf{H} \right\} dV \quad (9)$$

where V is the volume of the junction. The stationary point of the above functional is the unique solution of the problem, subject to the boundary conditions [21]

$$\mathbf{H} \times \mathbf{n} = 0 \quad \text{and} \quad \mathbf{H} \times \mathbf{n} = \mathbf{H}_0 \times \mathbf{n} \quad (10)$$

on perfect magnetic conductors and ports respectively. The integration along the x coordinate can be done analytically (see (1)); thus the volume integral in (9) reduces to a surface integral over the cross section Ω of the junction in the $y-z$ plane. The region Ω is divided into triangles, and the usual finite-element polynomial trial functions [22] are used for each component of the magnetic field. After the discretization of the functional (9) and applying the boundary conditions [23], the problem reduces to the equation

$$[W][H] = [b].$$

Here $[W]$ is an $N \times N$ real, symmetric matrix; $[H]$ is an $N \times 1$ matrix containing the values of the three components of the magnetic field at the nodes of the mesh; and $[b]$ is an $N \times 1$ matrix which results from the enforcement of the boundary conditions (10).

A P -port junction may be characterized by a $P \times P$ impedance matrix, which relates the normalized voltages and currents at the ports [24]. One of the strengths of the

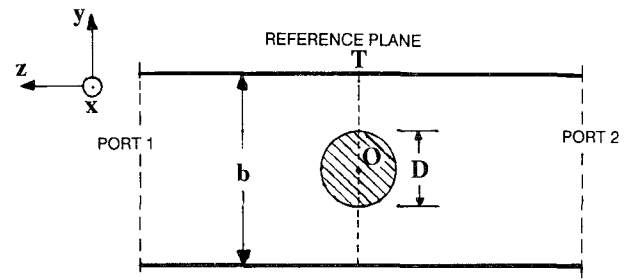


Fig. 3. Capacitive post (metallic or dielectric) in rectangular waveguide. The height of the waveguide is $b = 0.6$ m and the broad dimension of the waveguide is $a = 1.0$ m.

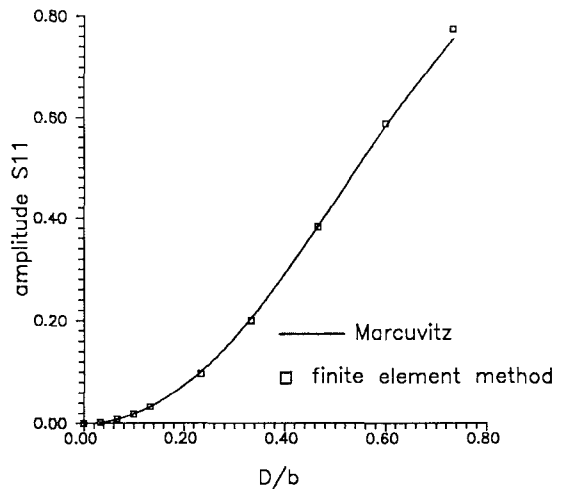


Fig. 4. Amplitude of the scattering coefficient S_{11} versus the metallic post diameter (refer to Fig. 3). The operating frequency is $k_0 = 41$ rads/m.

finite element method is that this impedance matrix can be found from the functional, which is a stationary quantity. Letting $\langle \cdot, \cdot \rangle$ be the bilinear form derived from (9) in the obvious manner, it may be shown that each entry of the impedance matrix is given by [23]

$$Z_{ij} = -j \frac{\eta_0}{k_0} \langle \mathbf{H}^{(i)}, \mathbf{H}^{(j)} \rangle, \quad i, j = 1, \dots, P \quad (11)$$

where η_0 is the impedance of free space and $\mathbf{H}^{(i)}$ is the computed magnetic field when port i is excited with unit current, the other $P-1$ ports being short-circuited. The calculation of the scattering matrix from the impedance matrix is straightforward [24].

The finite element program uses up to and including fourth-order polynomials. The program uses the precalculated K and L matrices [25] for fast matrix assembly and stores only the nonzero entries of the sparse global matrix. Some of the preprocessing and postprocessing work was done with existing packages [26].

IV. RESULTS

A. Metallic Post

Results for the centrally placed metallic post in Fig. 3 are shown in Figs. 4 and 5. Marcuvitz's equivalent circuit [1] is valid in the wavelength range $2b/\lambda_g < 1.0$, λ_g being

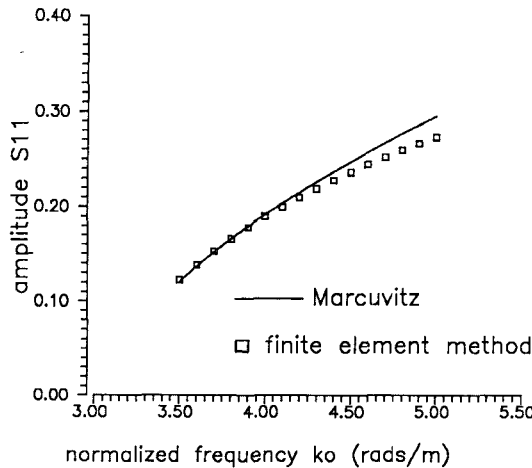


Fig. 5. Amplitude of the scattering coefficient S_{11} versus the normalized frequency k_0 . The ratio of the metallic post diameter to the height of the waveguide is $D/b = 0.333$ (refer to Fig. 3).

the guide wavelength. He estimated his expressions to be in error by a few percent in the range $D/b < 0.1$. Because of these limitations, his results diverge from our computed values for large posts (Fig. 4) and for higher frequencies (Fig. 5).

The structure in Fig. 3 has two symmetry planes:

- The symmetry plane T , which is also the reference plane for the results presented. (Because of this symmetry, solving the two-port junction is equivalent to solving two one-port half-problems [27].)
- The symmetry plane which passes through the center O of the junction and is parallel to the $x-z$ plane. This symmetry plane is an electric short circuit. Because of the two symmetries only one quarter of the region had to be modeled.

For the solution of the problem, approximately 190 finite elements were used, which were concentrated near the post where the field variations were expected to be the greatest. For a given ratio D/b and operating frequency k_0 and using second-order finite elements, the program ran for approximately 12 min on a Microvax II under the Ultrix operating system. The same problem solved with third-order elements (about double the number of degrees of freedom) gave scattering parameters which differed by about 0.1 percent from the second-order values, suggesting a high degree of convergence.

B. Dielectric Post

The only difference in the structure in this case is that the post consists of dielectric and has no metallic parts. The same symmetries apply. The region was divided into 205 finite elements. For a given ratio D/b and operating frequency k_0 and using second-order finite elements, the program ran for 18 min. Using third-order, the change in the scattering parameters was 0.2 percent. The results are shown in Figs. 6-9. Fig. 6 shows the $y-z$ part of the magnetic field. E_x was computed from \mathbf{H} using the ex-

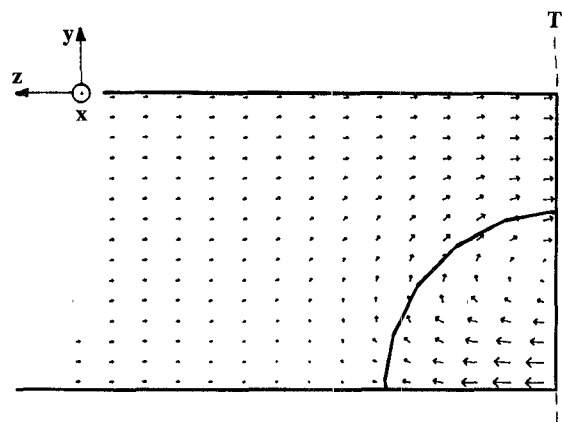


Fig. 6. The magnetic field distribution on the $y-z$ plane near the region of a dielectric post in a rectangular waveguide (refer to Fig. 3). The symmetry plane T is an open circuit. The relative permittivity is $\epsilon_r = 14.0$, and the normalized frequency $k_0 = 4.2$ rads/m. $D/b = 0.6$ (refer to Fig. 3).

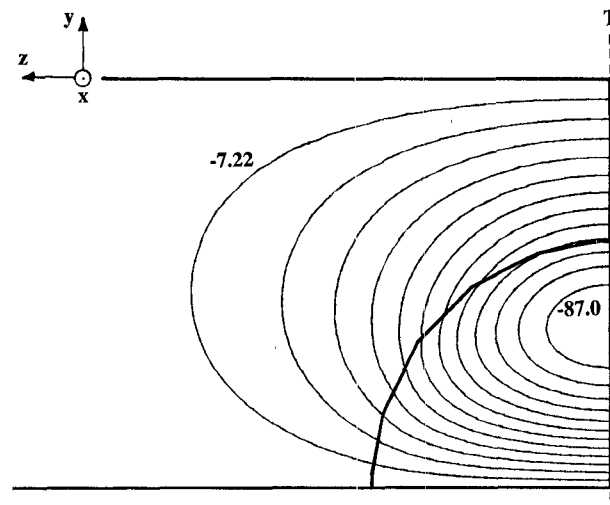


Fig. 7. Contour lines of E_x near a dielectric post in a rectangular waveguide (refer to Fig. 3). The symmetry plane T is an open circuit. The relative permittivity is $\epsilon_r = 14.0$, and the normalized frequency is $k_0 = 4.2$ rads/m. $D/b = 0.6$ (refer to Fig. 3). The numbers in the plot are the E_x values (V/m) of two of the equipotential lines.

pression

$$j\omega\epsilon_0\epsilon_r E_x = \frac{\partial H_z}{\partial y} - \frac{\partial H_y}{\partial z}.$$

Contour lines of E_x are shown in Fig. 7. Note that E_x is not zero near and within the dielectric object, even though it is nearly zero ($\sim 10^{-6}$ V/m) on the port, as expected. By contrast, the E_x computed for the metallic post was about 10^{-6} V/m everywhere.

We solved the problem using first-, second-, third-, and fourth-order finite elements. The convergence of our results is shown in Figs. 8 and 9. Note that the third-order results are almost the same as those of second order. The difference in the results between third and fourth order was negligible; therefore the fourth-order results are not shown. There is a significant error in first-order results at

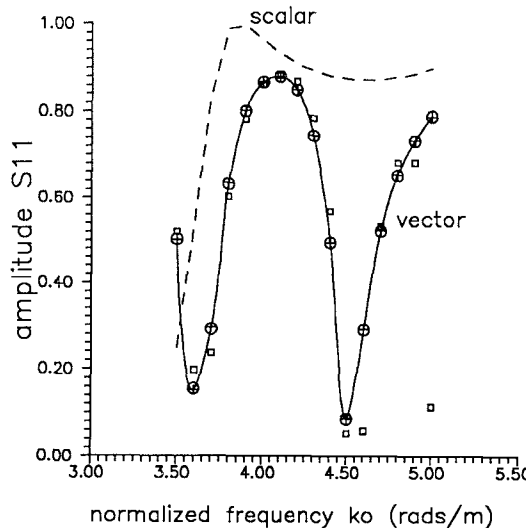


Fig. 8. Amplitude of the scattering coefficient S_{11} versus the normalized frequency k_0 . $D/b = 0.6$ (refer to Fig. 3). The relative permittivity is $\epsilon_r = 14.0$. The crosses are the calculated values of S_{11} using third-order finite elements and the solid line is an interpolation through those points. The circles and the squares are the calculated values using second- and first-order finite elements respectively. The dashed line is an interpolation through calculated values of S_{11} from scalar analysis using second-order finite elements.

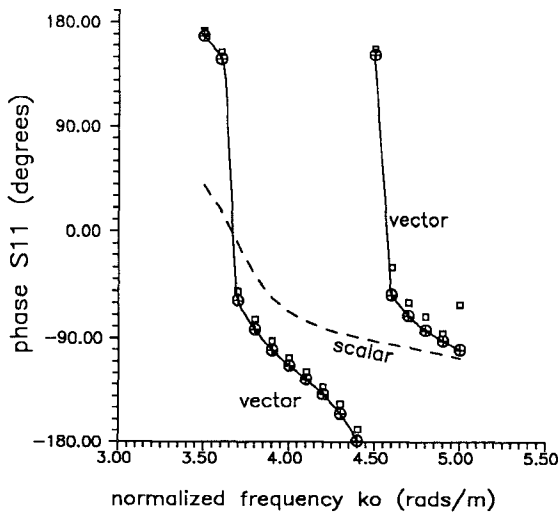


Fig. 9. Phase of the scattering coefficient S_{11} versus the normalized frequency k_0 . $D/b = 0.6$ (refer to Fig. 3). The relative permittivity is $\epsilon_r = 14.0$. The crosses are the calculated values of S_{11} using third-order finite elements and the solid line is an interpolation through those points. The circles and the squares are the calculated values using second- and first-order finite elements respectively. The junction shows inductive and capacitive behavior within the tested frequency range. The dashed line is an interpolation through calculated values of S_{11} from scalar analysis using second-order finite elements.

higher frequencies. This is because the variation of the field is bigger at higher frequencies and the elements are quite large compared to the guide wavelength. Fourth-order corresponds, approximately, to 6150 degrees of freedom, the third to 3500, the second to 1600, and the first to 450.

This problem was also analyzed with the scalar method using the functional given in [10] and second-order elements. The results are shown in Figs. 8 and 9 (dashed line). Note that the scalar method gives considerable errors. (The

same scalar method applied to the metallic post gave values identical to those obtained with the vector method, as expected.)

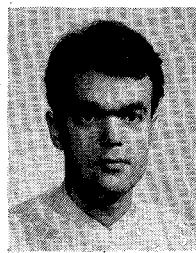
V. CONCLUSIONS

A complete finite element analysis for E -plane rectangular waveguide junctions has been presented. It was shown that E -plane problems can be analyzed as scalar problems (by solving for the H_x component of the magnetic field) only if one dielectric material is present in the junction. When different dielectric materials are present in the junction, the E_x component of the electric field is not zero and at least two variables, H_x and E_x , are required for the analysis. The new method solves for the three components of the magnetic field and finds the scattering parameters of the junction. Since it is a finite element analysis, the method can be used for arbitrarily shaped junctions with arrays of any number of metallic or dielectric posts, of arbitrary shape and location. For problems where previous results were available, the results obtained were found to be in very good agreement. In the case of dielectric post no previous results were available, but the convergence in the results as we moved from first to fourth order suggests that they are accurate.

REFERENCES

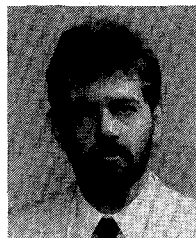
- [1] N. Marcuvitz, *Waveguide Handbook*. New York: McGraw-Hill, 1986.
- [2] J. P. Webb and S. Parihar, "Finite element analysis of rectangular waveguide problems," *Proc. Inst. Elec. Eng.*, vol. 133, pt. H, no. 2, pp. 91-94, Apr. 1986.
- [3] M. Koshiba, M. Sato, and M. Suzuki, "Application on finite-element method to H -plane waveguide discontinuities," *Electron. Lett.*, vol. 18, no. 9, p. 364-365, Apr. 1982.
- [4] M. Koshiba, M. Sato, and M. Suzuki, "Finite-element analysis of arbitrarily shaped H -plane waveguide discontinuities," *Trans. Inst. Electron. Commun. Eng. Japan (IECE)*, vol. E66, no. 2, pp. 82-87, Feb. 1983.
- [5] J. Schwinger and D. S. Saxon, *Discontinuities in Waveguides*. New York: Gordon and Breach, 1968, p. 60, lines 8-13.
- [6] J.-F. Lee and Z. J. Cendes, "An adaptive response modeling procedure for multiport microwave circuits," *IEEE Trans. Microwave Theory Tech.*, vol. MTT-35, pp. 1240-1247, Dec. 1987.
- [7] P. Silvester, "Finite element analysis of planar microwave networks," *IEEE Trans. Microwave Theory Tech.*, MTT-21, pp. 104-108, Feb. 1973.
- [8] G. D'Inzeo, F. Giannini, C. M. Sodi, and R. Sorrentino, "Method of analysis and filtering properties of microwave planar networks," *IEEE Trans. Microwave Theory Tech.*, vol. MTT-26, pp. 462-471, July 1978.
- [9] L. Lewin, "Reflection cancellation in waveguides—Junctions of uniform and tapered sections," *Wireless Eng.*, vol. 10, Aug. 1949.
- [10] M. Koshiba, M. Sato, and M. Suzuki, "Application of finite-element method to E -plane waveguide discontinuities," *Trans. Inst. Electron. Commun. Eng. Japan (IECE)*, vol. E66, no. 7, pp. 457-458, July 1983.
- [11] M. Koshiba and M. Suzuki, "Finite-element analysis of H -plane waveguide junction with arbitrarily shaped ferrite post," *IEEE Trans. Microwave Theory Tech.*, vol. MTT-34, pp. 103-109, Jan. 1986.
- [12] P. L. Carle, "New accurate and simple equivalent circuit for circular E -plane bends in rectangular waveguide," *Electron. Lett.*, vol. 23, no. 10, pp. 531-532, May 1987.
- [13] M. S. Leong, P. S. Kooi, and Chandra, "A new class of basis functions for the solution of the E -plane waveguide discontinuity problem," *IEEE Trans. Microwave Theory Tech.*, vol. MTT-35, pp. 705-709, Aug. 1987.

- [14] F. Arndt, I. Ahrens, U. Papziner, U. Wiechmann, and R. Wilkeit, "Optimized E-plane T-junction series power dividers," *IEEE Trans. Microwave Theory Tech.*, vol. MTT-35, pp. 1052-1059, Nov. 1987.
- [15] A. Okaya and L. F. Barash "The dielectric microwave resonator," *Proc. IRE*, vol. 50, pp. 2081-2092, Oct. 1962.
- [16] C. L. Ren, "Waveguide bandstop filter utilizing $\text{Ba}_2\text{Ti}_9\text{O}_{20}$ ceramics," in *IEEE MTT-S Int. Microwave Symp. Dig.*, June 1978, pp. 227-229.
- [17] C. G. Cox, "Waveguide power divider for satellite use," in *Proc. 3rd Int. Conf. Antennas Propagat.* (Norwich, England), 1983, pp. 341-343.
- [18] T. Yoneyama and S. Nishida, "Nonradiative dielectric waveguide T-junction for millimeter-wave applications," *IEEE Trans. Microwave Theory Tech.*, vol. MTT-33, pp. 1239-1241, Nov. 1985.
- [19] Y. Levitan and G. S. Sheaffer, "Analysis of inductive posts in rectangular waveguide," *IEEE Trans. Microwave Theory Tech.*, vol. MTT-35, pp. 48-59, Jan. 1987.
- [20] B. M. A. Rahman and J. B. Davies, "Finite-element analysis of optical and microwave waveguide problems," *IEEE Trans. Microwave Theory Tech.*, vol. MTT-32, pp. 20-28, Jan. 1984.
- [21] J. P. Webb, G. L. Maile, and R. L. Ferrari, "Finite-element solution of three-dimensional electromagnetic problems," *Proc. Inst. Elec. Eng.*, vol. 130, pt. H, no. 2, pp. 153-159, Mar. 1983.
- [22] P. P. Sylvester and R. L. Ferrari, *Finite Elements for Electrical Engineers*. New York: Cambridge University Press, 1983.
- [23] V. N. Kanellopoulos, "Vectorial finite element analysis of E-plane waveguide junctions," M. Eng. thesis, McGill University, Dec. 1987.
- [24] R. E. Collin, *Foundations of Microwave Engineering*. New York: McGraw-Hill, 1966.
- [25] P. Sylvester, "Construction of triangular finite element universal matrices," *Int. J. Number. Meth. Eng.*, vol. 12, pp. 237-244, 1978.
- [26] D. A. Lowther and P. P. Sylvester, *Computer-Aided Design in Magnetics*. New York: Springer-Verlag, 1986.
- [27] J. Helszajn, "Measurement of symmetrical waveguide discontinuities using the eigenvalue approach," *Proc. Inst. Elec. Eng.*, vol. 127, pt. H, no. 2, pp. 74-81, Apr. 1980.



Vassilios Kanellopoulos was born in Thessaloniki, Greece, in December 1962. He received the B.Sc. honours degree in physics from the Aristotle University of Thessaloniki, Greece, and the M.Eng. degree in electrical engineering from McGill University, Montréal, Canada, in 1985 and 1987 respectively. Currently he is pursuing the Ph.D. degree in electrical engineering at McGill. His work focuses on the numerical simulation of vector three-dimensional open boundary electromagnetic problems using the finite element method. His research interests include numerical high-frequency electromagnetics with application to biomedical problems.

+



J. P. Webb (M'83) received the Ph.D. degree from Cambridge University, England, in 1981.

Since 1982 he has been an Assistant Professor, then an Associate Professor, in the Electrical Engineering Department of McGill University, Montréal, Canada. His area of research is computer methods in electromagnetics, especially the application of the finite element method.